



RESEARCH ARTICLE

An External Matrix-Assisted Laser Desorption Ionization Source for Flexible FT-ICR Mass Spectrometry Imaging with Internal Calibration on Adjacent Samples

Donald F. Smith,¹ Konstantin Aizikov,² Marc C. Duursma,¹ Frans Giskes,¹
Dirk-Jan Spaanderman,¹ Liam A. McDonnell,^{1,3} Peter B. O'Connor,^{2,4}
Ron M. A. Heeren¹

¹FOM Institute for Atomic and Molecular Physics, Science Park 104, 1098 XG Amsterdam, The Netherlands

²Mass Spectrometry Resource, Department of Biochemistry, Boston University School of Medicine, Boston, MA, USA

³Department of Parasitology, Leiden University Medical Center, P.O. Box 9600, 2300 RC Leiden, The Netherlands

⁴Department of Chemistry, University of Warwick, Coventry, UK

Abstract

We describe the construction and application of a new MALDI source for FT-ICR mass spectrometry imaging. The source includes a translational X-Y positioning stage with a 10 × 10 cm range of motion for analysis of large sample areas, a quadrupole for mass selection, and an external octopole ion trap with electrodes for the application of an axial potential gradient for controlled ion ejection. An off-line LC MALDI MS/MS run demonstrates the utility of the new source for data- and position-dependent experiments. A FT-ICR MS imaging experiment of a coronal rat brain section yields ~200 unique peaks from m/z 400–1100 with corresponding mass-selected images. Mass spectra from every pixel are internally calibrated with respect to polymer calibrants collected from an adjacent slide.

Key words: Fourier transform, Ion cyclotron resonance, FTMS, Imaging mass spectrometry, INCAS

Introduction

Mass spectrometry (MS) imaging combines molecular (mass) information with spatial information from complex surfaces (e.g., biological tissues) [1–3]. Current instrumental and method developments aim to improve one or both of these facets. Time-of-flight secondary-ion mass spectrometry (TOF-SIMS), stigmatic matrix-assisted laser desorption ionization (MALDI)-TOF ion microscope and highly focused microprobe experiments (via MALDI or SIMS) allow high spatial resolution to sub-micrometer scale [4–13]. On the other hand, high-performance mass spec-

trometers (e.g., Fourier transform ion cyclotron resonance (FT-ICR) mass spectrometers [14] and hybrid linear ion trap (LTQ)-Orbitrap [15], which shall be inclusively referred to as “FT”) are now being used for complementary high mass resolving power and high mass accuracy MS for identification of observed species [16–19]. Here, instrumentation and methodology for a custom-built MALDI source for FT-ICR mass spectrometry imaging are described.

Laser microprobe systems represent the earliest chemical imaging utilizing FT-ICR MS. Early systems used in-cell laser desorption ionization (LDI) for profiling and imaging experiments, with imaging experiments typically in one dimension (i.e., line scans) [20–23]. While these systems generally had excellent spatial resolution, easily less than 10 μm laser spot diameter, the species analyzed were

Correspondence to: Ron M. A. Heeren; e-mail: heeren@amolf.nl

typically less than m/z 500 and were comprised of mainly metals and metal oxides. These systems relied on sophisticated optics for alignment of the laser beam inside the vacuum system and the operation of a translational stage within the bore of a superconducting magnet was a challenge. However, one such system is currently being used for geomatrix-assisted laser desorption/ionization MS imaging of rock/mineral samples [24].

Ease of access is arguably the largest disadvantage of in-cell ionization techniques. Thus, external laser microprobe ion sources were developed which alleviated some of the above mentioned challenges [25, 26]. Concurrently, the development of MALDI [27–30] for analysis of intact biomolecules by FT-ICR MS was also receiving considerable attention, owing to the advantages of FT-ICR MS over TOF instruments. Many in-cell MALDI FT-ICR systems were developed, though none for MS imaging [31–35]. The development of external MALDI ion sources, typically with the extraction of ions into a multipole storage device, allowed easy access for changing samples and opened the door for higher-throughput MALDI FT-ICR MS [36–43]. Translational X-Y stages addressed the need for large sample plate loading for multi-sample analysis, and these were installed in systems with extraction of ions into a multipole, as described above [44, 45]. The external MALDI source described in this paper is similar in design, with extraction of MALDI-generated ions into a hexapole ion guide and subsequent transfer to a storage octopole. The new Bruker Apollo II dual ESI/MALDI source, which is equipped for MS imaging studies, utilizes a dual ion funnel for collection and focusing of MALDI-generated ions before storage in an external multipole ion trap.

The utility of MALDI FT-ICR for the direct analysis of biological tissues has been demonstrated for peptides from crab neurons [46], crab sinus glands [47], and a wide array of decapod neural tissues [48, 49]. Further, MALDI FT-MS imaging has been used to image peptides and lipids in rat and mouse brain [16, 19, 50] and drugs and metabolites from rat kidney and liver, as well as mouse brain [17]. These studies demonstrate the need for high mass resolving power to resolve isobaric ions and the advantage of high mass accuracy for the identification of analytes and MS/MS fragments.

The instrument described herein presents a flexible platform for high mass resolution and high mass accuracy FT-ICR mass spectrometry imaging. The capabilities of this custom-built instrument—such as workflow-based control software [51, 52], easy implementation of different ICR cell designs [53], and fragmentation by simultaneous electron-capture dissociation infrared multiphoton dissociation (ECD/IRMPD) [54]—expand the possibilities of FT-ICR MS imaging; such possibilities are otherwise not easily implemented on commercial systems.

A liquid chromatography (LC)-MALDI experiment was “imaged” to test the new configuration in a data- and

position-dependent MS/MS mode. Half of a coronal rat brain section was imaged to assess the applicability of the system to tissue analysis, where over 200 unique peaks are observed. Polymer calibrant ions are collected from an adjacent glass slide and provide internal calibration over the entire dataset, thus bypassing any difficulties associated with ion suppression following the deposition of calibrants on the tissue surface. In addition, internal calibration of each pixel of the imaging experiment allows confident generation of mass-selected images with narrow (10 mDa) mass windows. In-house developed software is used to produce high mass resolution “datacubes” for easy data navigation and analysis.

Materials and Methods

Sample Preparation

LC-MALDI Acetonitrile (BioSolve, Valkenswaard, NL) and acetic acid (JT Baker, Phillipsburg, NJ, USA) were used without prior purification. Savinase (synthetic bacillus serine protease) was digested with trypsin and CNBr and 5 μ L was separated on a LC Packings nanoLC-system (Dionex, Amsterdam, NL) with a C18 PepMap 100 pre-column (internal diameter 300 μ m, length 1 mm) and a C18 PepMap 100 analytical column (internal diameter 75 μ m, length 15 cm). The eluents were 0.1% formic acid and 5% acetonitrile in water (A) and 0.1% formic acid and 5% water in acetonitrile (B). The LC method was 50 min with an initial 6 min equilibrium period, followed by a gradient of 20 min 0–70% B, a 1 min gradient of 70–95% B, 10 min of 95% B, and 13 min of 5% B. The capillary was coupled to a Symbiot I sample workstation (Applied Biosystems, Foster City, CA, USA) and effluent was spotted at intervals of 30 s and a spacing of 1 mm (10 \times 10 matrix) on a pre-made 2,5-dihydroxybenzoic acid (DHB) MALDI foil (LabConnections, Northborough, MA, USA). The delay time between the start of the LC run and spot deposition was 20 min. Peptide and protein were identified by Mascot database search (www.matrixscience.com).

Rat Brain Section and Polymer Calibrants A 12 μ m thick coronal section of rat brain (Harlan Laboratories, Boxmeer, The Netherlands) was prepared in a Microm HM 525 cryomicrotome (Microm International, Walldorf, Germany) at -20 $^{\circ}$ C and placed on indium–tin oxide coated glass slides (ITO, 4–8 Ω resistance; Delta Technologies, Stillwater, MN). The section was washed with cold (-20 $^{\circ}$ C) ethanol (70% in H₂O) and coated with \sim 30 layers of a 30 mg/mL solution (1:1 MeOH/H₂O (0.2% trifluoroacetic acid)) of DHB with a Bruker ImagePrep matrix deposition device. For internal calibration, an \sim 156 μ M solution of poly(methyl methacrylate) 640 (PMMA) was prepared in a 30 mg/mL solution of DHB and deposited on an ITO-coated glass slide as described above. Lipid assignments were made using LIPID MAPS (LIPID Metabolites and Pathways Strategy; <http://www.lipidmaps.org>)

with a mass tolerance of 0.01 Da with regards to the average measured mass.

Instrumentation

All experiments were performed on a heavily modified Bruker APEX 7.0e FT-ICR mass spectrometer [55]. Figure 1 shows a schematic of the new instrument configuration. A 355 nm Nd:YAG laser (1000 Hz repetition rate; Bright-Solutions, Cura Carpignano, Italy) is coupled to the source through a 3 m tapered fiber optic cable (800–200 μm , Fiberguide Industries, Stirling, NJ, USA). The beam is collimated after the fiber optic cable and aligned through the hexapole rods and conductance limit (4 mm) onto the sample surface, which is ~ 2 mm from the hexapole entrance. The laser power, start time, and output frequency are controlled from the data station. In addition, a 337 nm N_2 laser (Laser Science, Inc., Franklin, MA, USA) can also be coupled to the system. A translational X-Y stage with 10×10 cm range of motion (Fraunhofer USA, Brookline, MA, USA) allows for the analysis of large sample areas [56]. For ESI, the MALDI stage is removed and replaced with an electrodynamic ion funnel [57–59] and operated in nano-ESI mode.

For MALDI analysis, the source chamber is $\sim 5 \times 10^{-5}$ mbar and a small (0.5–5 V) positive bias voltage is applied to the sample plate (over the hexapole entrance conductance limit). Ions from the surface pass through the hexapole conductance limit and are injected into a short (75 mm) transfer hexapole, pass through a mass-selective quadrupole (ABB Extrel, Pittsburg, PA, USA) before storage (0.1–1 s) in a 170 mm accumulation octopole (with helium cooling gas at $\sim 5 \times 10^{-6}$ mbar) [60]. External ion accumulation allows for the accumulation of a large number of laser shots at high repetition rate. In addition, calibrants from an adjacent sample [61, 62] can be stored in the octopole while analyte ions are collected, and the entire packet sent to the ICR cell simultaneously. Ejection electrodes are used

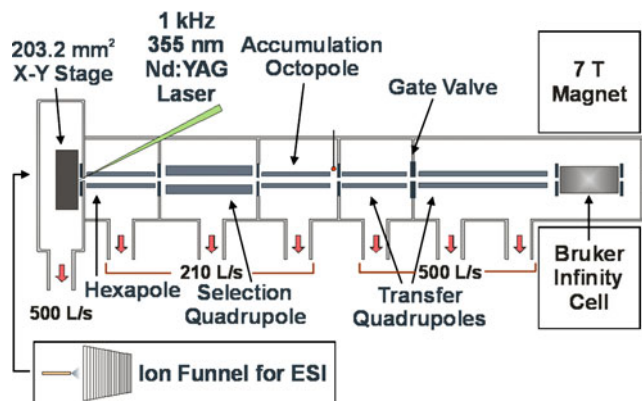


Figure 1. Schematic of the AMOLF 7 Tesla MALDI/ESI FT-ICR mass spectrometer. The source features an X-Y stage with 10×10 cm range of motion for MALDI that can be replaced with an electrodynamic ion funnel for ESI

for efficient extraction of ions into two transfer quadrupoles (253 and 889 mm) (ABB Extrel, Pittsburg, PA) [63, 64]. This improves image contrast by increasing the number of ions observed per pixel and thus the detection efficiency. The instrument can be equipped with either a capacitively coupled cylindrical open ICR cell [53] or a Bruker Infinity cell [65], where ions are cooled with an argon pulse gas [66] before broadband frequency (chirp) excitation [67] and direct-mode detection. An in-house developed workflow-based data station (“AWG3”) is used for experiment control and data acquisition [51, 52].

Results and Discussion

The new source was designed around an X-Y translational stage with high position accuracy ($<0.4 \mu\text{m}$), with a 10×10 cm range of motion for analysis of large samples. The AWG3 workflow-based data station uses command and decision modules, which are termed “nodes”, for easy and flexible design of FT-ICR experiments. Stage control is managed through a new “StageDriver” node in the AWG3 flow-based control software. The absolute position of the sample stage is calibrated by a simple three-point (or more) calibration routine of the sample stage live feed with respect to a scan of the sample plate. Regions of interest with user-defined raster size can be defined by polygonal or rectangular grids. “Stage command” nodes in the workflow define stage movements such as an offset relative to the current position, a “go to position” command, and a decision to wait for the stage to stop movement. The stage position is stored as a variable and can be used for position-dependent experiments. An overview of alternative MS imaging control software for FT and time-of-flight MALDI instruments can be found elsewhere [68].

Figure 2 shows a data-dependent (LC)-MALDI FT-ICR MS/MS “imaging” experiment of a trypsin/CNBr digest of savinase. An optical image of the spotted MALDI foil with an overlay of the UV LC trace is shown in Figure 2a. Mass-selected images of three tryptic peptides are shown in Figure 2b and an overlay of m/z 1200.8464 (red; NPSWSNVQIR) and its y8 product ion (m/z 989.6202, blue; SWSNVQIR) are shown in Figure 2c. Mascot database search resulted in a Mowse probability score of 72 with 45% sequence coverage. The workflow for the (LC)-MALDI LC-MS/MS experiment is shown in Figure 2d. Here, a prescan was collected and evaluated by the *PeakPicker* node to determine if peaks were present, followed by declustering to mono-isotopic peaks in the *ClusterList* node. If at least one cluster was found, the stage was offset and the ion corresponding to the most abundant peak from the prescan was isolated by stored waveform inverse Fourier transform (SWIFT) [69] and fragmented by sustained off-resonance irradiation collision-induced dissociation (SORI-CID) [70, 71]. This workflow can be modified to fragment specific target ions (i.e., a selected reaction monitoring experiment) or

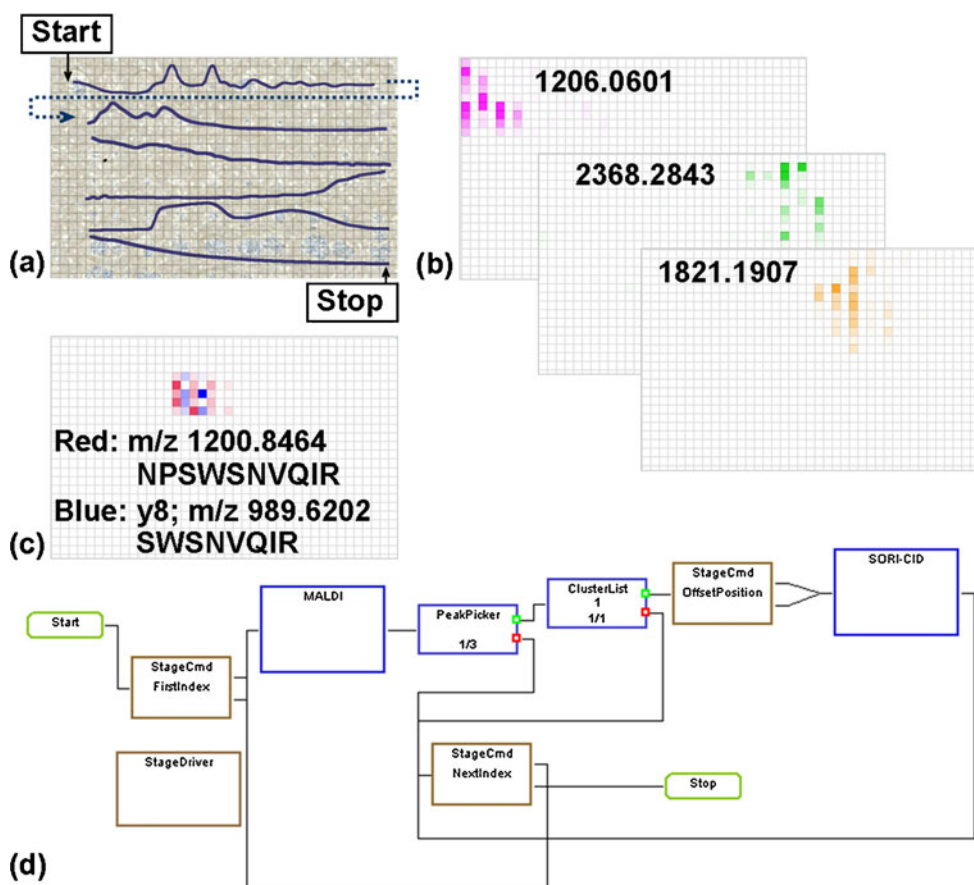


Figure 2. Positive-ion MALDI FT-ICR MS/MS experiment of synthetic bacillus serine protease (savinase). (a) LC UV trace overlaid with optical image of effluent spotted pre-made MALDI foil. (b) FT-ICR MS “images” for selected peptides and (c) parent (red, m/z 1200.8464) and y_8 fragment (blue, m/z 989.6202) of the tryptic peptide NPSWSNVQIR. The grid indicates the raster positions of 300 μm . (d) The data-dependent workflow used for the LC MALDI run

to store the mass of fragmented ions to ensure the same ion is not fragmented multiple times.

Careful mass calibration is essential for confident generation of mass-selected images from large MS imaging and LC-MALDI datasets. This is especially important for MALDI MS imaging, where the shot-to-shot variation of MALDI, compounded with the spatial variations in analytes concentration on the tissue surface, lead to ion number variations in the ICR cell which shift the measured frequency (and thus the mass) [72–75]. Calibration methods used for MALDI FT-MS imaging include internal calibration on MALDI matrix clusters [17] and lock mass calibration on a known m/z [76].

The MALDI source described herein exhibits no MALDI matrix interferences, so internal calibration by these means is not possible. In addition, the system does not have the ability to closely control the number of ions injected into the ICR cell (i.e., automatic gain control [77–81]). Thus, a strategy for internal calibration on adjacent samples (INCAS) [61, 62] was developed to allow confident internal calibration on *every* pixel of the dataset. Figure 3 shows a representative workflow for the INCAS strategy. First, internal calibrants (here, PMMA 640) are collected from an adjacent slide and stored in the external

octopole ion trap. The X-Y stage is moved to the sample where analytes are collected and stored in the same external octopole ion trap. Thus, both calibrants and analytes can be sent to the ICR cell simultaneously, and

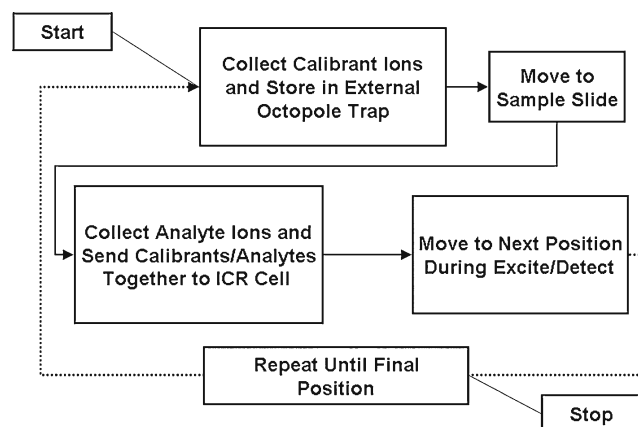


Figure 3. INCAS strategy for a FT-ICR MS imaging experiment. The collection of calibrants from an adjacent slide avoids ion-suppression effects that are possible when the calibrant is applied directly on the tissue

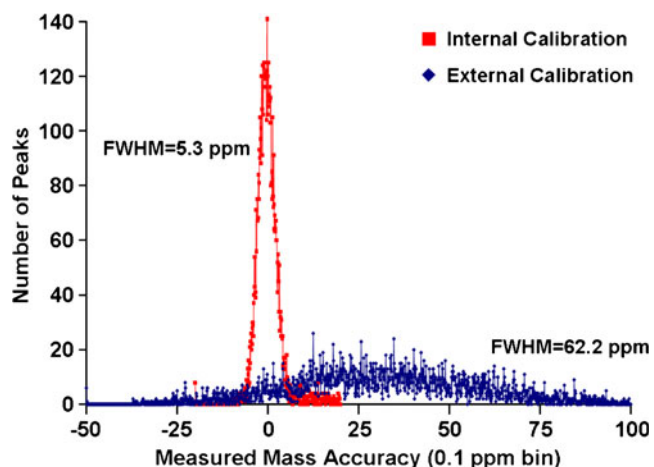


Figure 4. Number of peaks per bin *versus* mass measurement accuracy (0.1 ppm bin size) for six lipids (m/z 760, 767, 772, 782, 798, and 804) observed in rat brain ($N_{\text{peaks}}=7499$). Internal calibration centers the distribution around zero and narrows the FWHM

ion suppression due to the application of calibrants on the sample can be avoided. Here, the application of PMMA 640 on tissue (in the MALDI matrix solution) resulted in no signal for either the polymers or tissue analytes. However, peptide standards applied directly on tissue may prove useful as internal calibrants. In-house data analysis software was used to locate calibrant peaks and to calculate and apply the internal calibration parameters [74].

A rat brain coronal section was used to test the tissue imaging capabilities of the new source to which the INCAS strategy was applied. Figure 4 shows the result of internal calibration for *every* pixel from a FT-ICR MS imaging experiment of half of the rat brain section. The measured mass accuracies (in parts per million (ppm)) of six common glycerophospholipids (with phosphocholine (PC) and glycerophosphate (PA) head groups) observed in brain [19, 82–86], m/z 760 ([PC 34:1+H]⁺), 767 ([PA 38:2+K]⁺, 772 ([PC 32:0+K]⁺), 782 ([PC 34:1+Na]⁺), 798 ([PC 34:1+K]⁺), and 804 ([PC 36:4/PE 39:4+Na]⁺) were calculated, binned into

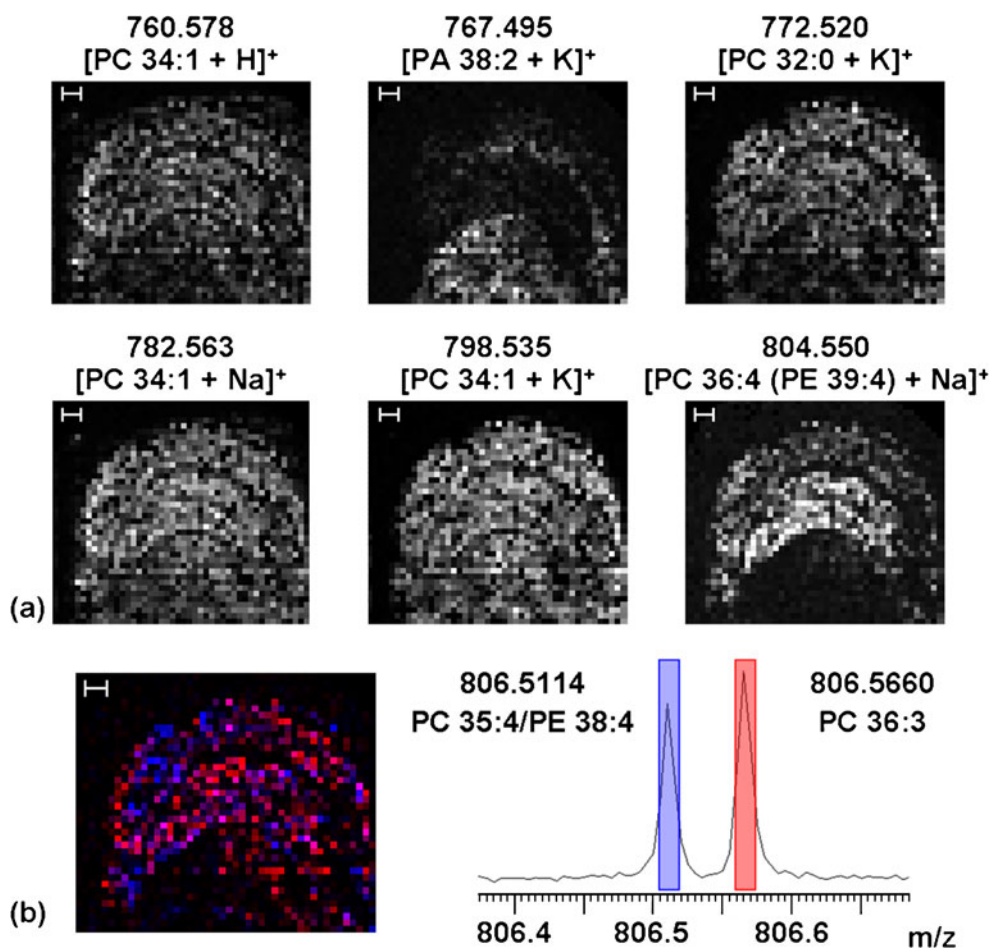


Figure 5. (a) Mass-selected images of six lipids from a positive-ion MALDI FT-ICR MS imaging experiment of a coronal rat brain section collected at 200 μm raster size. The images are from the range of the stated mass ± 0.01 Da (e.g., 760.578–760.588). Scale bar=600 μm . (b) Overlay and datacube mass spectrum of two isobaric ions at m/z 806. Blue=806.5114 and red=806.5660. The width of the colored bars indicates the mass range selected for the overlaid images. Pink pixels indicate where these two ions are observed in the same pixel

0.1 m/z bins, and plotted as histograms for internal and externally calibrated datasets. Internal calibration greatly improves the measured mass accuracy and narrows the full width at half-maximum (FWHM) of the histogram, which allows for smaller mass windows for generation of mass-selected images, such as those shown in Figure 5a for these six lipids.

In addition, ~200 unique peaks ($S/N > 5:1$) were observed from m/z 400–1100, with an average mass resolving power ($m/\Delta m_{50\%}$) of 122,000. In-house developed software was used to create a datacube of the X-Y correlated mass spectra, in which data can be easily navigated and mass-selected images exported [87]. The large number of spectra from an FT-ICR MS imaging experiment, here 1777, requires mass spectral binning in order to reduce the datacube size; here, a bin size of 0.005 Da was used (as determined by the FWHM of the internal calibration shown in Figure 4, where 5 ppm at mass 700 is 0.0035, to ensure small shifts in mass do not distort the peak shape in the datacube binned mass spectrum). The spectra and the red-blue overlay in Figure 5b show two isobaric ions at m/z 806 which have different spatial distributions (blue = 806.5114 (PC 35:4/PE 38:4) and red = 806.5660 (PC 36:3)). The high mass resolving power of FT-ICR MS easily resolves these two ions which differ in mass by ~55 mDa. In addition, the high mass accuracy allows confident assignment of elemental compositions and identifies these peaks as corresponding to distinct glycerophospholipid species. Long detection times for high-resolution FT-MS imaging remain the time-limiting step. Here, transients of 2.6 s (in addition to pulse-gas pump-down delay) were collected in a serial fashion, which presents a significantly longer image acquisition time over MALDI TOF instruments. The move to higher-field superconducting magnets for FT-ICR [88], higher-performance electrostatic FT instruments [89], and interlaced data acquisition strategies (e.g., the collection of analytes during the excite/detect events) will improve the duty cycle for FT-MS imaging studies.

Conclusions

We have constructed a dedicated MALDI source for FT-ICR mass spectrometry imaging. Software updates allow data- and position-dependent workflow-based MS imaging experiments as demonstrated with a (LC)-MALDI MS/MS experiment. Mass-resolved images of lipids from a rat brain section demonstrate the utility of the new source for biological tissue measurements. INCAS allows confident mass assignment without adulteration of the sample surface with calibrants. Isobaric ions with a mass difference of ~55 mDa are mass resolved (over the entire mass spectrum) and display different spatial distributions.

Acknowledgment

This work is part of the research program of the “Stichting voor Fundamenteel Onderzoek der Materie (FOM)”, which

is financially supported by the “Nederlandse organisatie voor Wetenschappelijk Onderzoek (NWO)”. This project is part of the E.U. project COMPUTIS, 6th European Framework Program for Research and Technological Development (FP6), project no. LSHG-CT-2005-5181194. In addition, this work was also funded by the E.U. project MEDITRANS and the Netherlands Proteomics Centre. We thank Tzu-Yung (Terry) Lin, David Chargin, and Sergei Ivanov from Fraunhofer CMI for technical help with the translational stage. K.A. thanks David H. Perlman, Cheng Lin, Nadezda Sargaeva, and Chunxiang Yao from Boston University for support and helpful discussions.

Open Access

This article is distributed under the terms of the Creative Commons Attribution Noncommercial License which permits any noncommercial use, distribution, and reproduction in any medium, provided the original author(s) and source are credited.

References

1. Reyzer, M.L., Caprioli, R.M.: MALDI-MS-based imaging of small molecules and proteins in tissues. *Curr. Opin. Chem. Biol.* **11**(1), 29–35 (2007)
2. McDonnell, L.A., Heeren, R.M.A.: Imaging mass spectrometry. *Mass Spectrom. Rev.* **26**(4), 606–643 (2007)
3. Heeren, R.M.A., Smith, D.F., Stauber, J., Kukrer-Kaletas, B., MacAleese, L.: Imaging mass spectrometry: hype or hope? *J. Am. Soc. Mass Spectrom.* **20**(6), 1006–1014 (2009)
4. Chandra, S., Smith, D.R., Morrison, G.H.: Subcellular imaging by dynamic SIMS ion microscopy. *Anal. Chem.* **72**(3), 104a–114a (2000)
5. Chandra, S.: SIMS ion microscopy as a novel. Practical tool for subcellular chemical imaging in cancer research. *Appl. Surf. Sci.* **203**, 679–683 (2003)
6. McDonnell, L.A., Piersma, S.R., Altelaar, A.F.M., Mize, T.H., Luxembourg, S.L., Verhaert, P.D.E.M., van Minnen, J., Heeren, R.M.A.: Subcellular imaging mass spectrometry of brain tissue. *J. Mass Spectrom.* **40**(2), 160–168 (2005)
7. Altelaar, A.F.M., van Minnen, J., Jimenez, C.R., Heeren, R.M.A., Piersma, S.R.: Direct molecular imaging of *lymnaea stagnalis* nervous tissue at subcellular spatial resolution by mass spectrometry. *Anal. Chem.* **77**(3), 735–741 (2005)
8. Altelaar, A.F.M., Klinkert, I., Jalink, K., de Lange, R.P.J., Adan, R.A.H., Heeren, R.M.A., Piersma, S.R.: Gold-enhanced biomolecular surface imaging of cells and tissue by SIMS and MALDI mass spectrometry. *Anal. Chem.* **78**(3), 734–742 (2006)
9. Arlinghaus, H.F., Kriegeskotte, C., Fartmann, M., Wittig, A., Sauerwein, W., Lipinsky, D.: Mass spectrometric characterization of elements and molecules in cell cultures and tissues. *Appl. Surf. Sci.* **252**(19), 6941–6948 (2006)
10. Altelaar, A.F.M., Luxembourg, S.L., McDonnell, L.A., Piersma, S.R., Heeren, R.M.A.: Imaging mass spectrometry at cellular length scales. *Nat. Protoc.* **2**(5), 1185–1196 (2007)
11. Chaurand, P., Schriver, K.E., Caprioli, R.M.: Instrument design and characterization for high resolution MALDI-MS imaging of tissue sections. *J. Mass Spectrom.* **42**(4), 476–489 (2007)
12. Fletcher, J.S., Rabbani, S., Henderson, A., Blenkinsopp, P., Thompson, S.P., Lockyer, N.P., Vickerman, J.C.: A new dynamic in mass spectral imaging of single biological cells. *Anal. Chem.* **80**(23), 9058–9064 (2008)
13. Nie, H.Y., Francis, J.T., Taylor, A.R., Walzak, M.J., Chang, W.H., MacFabe, D.F., Lau, W.M.: Imaging subcellular features of a sectioned rat brain using time-of-flight secondary ion mass spectrometry and scanning probe microscopy. *Appl. Surf. Sci.* **255**(4), 1079–1083 (2008)
14. Marshall, A.G., Hendrickson, C.L., Jackson, G.S.: Fourier transform ion cyclotron resonance mass spectrometry: a primer. *Mass Spectrom. Rev.* **17**(1), 1–35 (1998)
15. Makarov, A.: Electrostatic axially harmonic orbital trapping: a high-performance technique of mass analysis. *Anal. Chem.* **72**(6), 1156–1162 (2000)

16. Taban, I.M., Altelaar, A.F.M., Van der Burgt, Y.E.M., McDonnell, L.A., Heeren, R.M.A., Fuchser, J., Baykut, G.: Imaging of peptides in the rat brain using MALDI-FTICR mass spectrometry. *J. Am. Soc. Mass Spectrom.* **18**(1), 145–151 (2007)
17. Cornett, D.S., Frappier, S.L., Caprioli, R.M.: MALDI-FTICR imaging mass spectrometry of drugs and metabolites in tissue. *Anal. Chem.* **80**(14), 5648–5653 (2008)
18. Landgraf, R.R., Prieto Conaway, M.C., Garrett, T.J., Stacpoole, P.W., Yost, R.A.: Imaging of lipids in spinal cord using intermediate pressure matrix-assisted laser desorption-linear ion trap/Orbitrap MS. *Anal. Chem.* **81**(20), 8488–8495 (2009)
19. Pól, J., Vidová, V., Kruppa, G., Koblíha, V., Novák, P., Lemr, K., Kotiaho, T., Kostianinen, R., Havlíček, V., Volný, M.: Automated ambient desorption-ionization platform for surface imaging integrated with a commercial Fourier transform ion cyclotron resonance mass spectrometer. *Anal. Chem.* **81**(20), 8479–8487 (2009)
20. Pelletier, M., Kreier, G., Muller, J.F., Weil, D., Johnston, M., Marshall, A.G.: Laser microprobe Fourier transform mass spectrometry. preliminary results for feasibility and evaluation. *Rapid Commun. Mass Spectrom.* **2**(7), 146–150 (1988)
21. Brenna, J.T., Creasy, W.R., McBain, W., Soria, C.: Nd-YAG laser microprobe system for Fourier-transform ion-cyclotron resonance mass-spectrometry. *Rev. Sci. Instrum.* **59**(6), 873–879 (1988)
22. Behm, J.M., Hemminger, J.C., Lykke, K.R.: Microscopic laser desorption postionization Fourier transform mass spectrometry. *Anal. Chem.* **68**(5), 713–719 (1996)
23. Scott, J.R., Tremblay, P.L.: Highly reproducible laser beam scanning device for an internal source laser desorption microprobe Fourier transform mass spectrometer. *Rev. Sci. Instrum.* **73**(3), 1108–1116 (2002)
24. Richardson, C.D., Hinman, N.W., McJunkin, T.R., Kotler, J.M., Scott, J.R.: Exploring biosignatures associated with thenardite by geomatrix-assisted laser desorption/ionization Fourier transform ion cyclotron resonance mass spectrometry (MALDI-FTICR-MS). *Geomicrobiol. J.* **25**(7–8), 432–440 (2008)
25. Vanvaeck, L., Vanroy, W., Struyf, H., Adams, F., Caravatti, P.: Development of a laser microprobe Fourier-transform mass-spectrometer with external ion-source. *Rapid Commun. Mass Spectrom.* **7**(5), 323–331 (1993)
26. Struyf, H., Van Roy, W., Van Vaeck, L., Van Grieken, R., Gijbels, R., Caravatti, P.: Laser microprobe Fourier transform mass spectrometer with external ion source for organic and inorganic microanalysis. *Anal. Chim. Acta* **283**(1), 139–151 (1993)
27. Karas, M., Bachmann, D., Bahr, U., Hillenkamp, F.: Matrix-assisted ultraviolet laser desorption of non-volatile compounds. *Int. J. Mass Spectrom. Ion Process.* **78**, 53–68 (1987)
28. Karas, M., Bahr, U., Hillenkamp, F.: UV laser matrix desorption ionization mass-spectrometry of proteins in the 100 000 dalton range. *Int. J. Mass Spectrom. Ion Process.* **92**, 231–242 (1989)
29. Hillenkamp, F., Karas, M., Beavis, R.C., Chait, B.T.: Matrix-assisted laser desorption ionization mass-spectrometry of biopolymers. *Anal. Chem.* **63**(24), A1193–A1202 (1991)
30. Berkenkamp, S., Kirpekar, F., Hillenkamp, F.: Infrared MALDI mass spectrometry of large nucleic acids. *Science* **281**(5374), 260–262 (1998)
31. Nuwaysir, L.M., Wilkins, C.L., Simonsick, W.J.: Analysis of copolymers by laser desorption Fourier-transform mass-spectrometry. *J. Am. Soc. Mass Spectrom.* **1**(1), 66–71 (1990)
32. Cornett, D.S., Duncan, M.A., Amster, I.J.: Matrix-assisted laser desorption at visible wavelengths using a 2-component matrix. *Org. Mass Spectrom.* **27**(7), 831–832 (1992)
33. Castoro, J.A., Wilkins, C.L.: Ultrahigh-resolution matrix-assisted laser-desorption ionization of small proteins by Fourier-transform mass-spectrometry. *Anal. Chem.* **65**(19), 2621–2627 (1993)
34. Smith, E.T., Cornett, D.S., Amster, I.J., Adams, M.W.W.: Protein molecular-weight determinations by MALD mass-spectrometry: a superior alternative to gel-filtration. *Anal. Biochem.* **209**(2), 379–380 (1993)
35. Easterling, M.L., Pitsenberger, C.C., Kulkarni, S.S., Taylor, P.K., Amster, I.J.: A 4.7 Tesla internal MALDI-FTICR instrument for high mass studies: performance and methods. *Int. J. Mass Spectrom. Ion Process.* **157–158**, 97–113 (1996)
36. Li, Y.Z., McIver, R.T.: Detection limits for matrix-assisted laser-desorption of polypeptides with an external ion-source Fourier-transform mass-spectrometer. *Rapid Commun. Mass Spectrom.* **8**(9), 743–749 (1994)
37. McIver, R.T., Li, Y.Z., Hunter, R.L.: High-resolution laser-desorption mass-spectrometry of peptides and small proteins. *Proc. Natl Acad. Sci. U.S.A.* **91**(11), 4801–4805 (1994)
38. de Koster, C.G., Duursma, M.C., van Rooij, G.J., Heeren, R.M.A., Boon, J.J.: Endgroup analysis of polyethylene glycol polymers by matrix-assisted laser desorption/ionization Fourier-transform ion cyclotron resonance mass spectrometry. *Rapid Commun. Mass Spectrom.* **9**(10), 957–962 (1995)
39. Heeren, R.M.A., Boon, J.J.: Rapid microscale analyses with an external ion source Fourier transform ion cyclotron resonance mass spectrometer. *Int. J. Mass Spectrom.* **157**, 391–403 (1996)
40. O'Connor, P.B., Duursma, M.C.: vanRooij, G. J., Heeren, R. M. A. Boon, J. J.: Correction of time-of-flight shifted polymeric molecular weight distributions in matrix assisted laser desorption/ionization Fourier transform mass spectrometry. *Anal. Chem.* **69**(14), 2751–2755 (1997)
41. Green, M.K., Medforth, C.J., Muzzi, C.M., Nurco, D.J., Shea, K.M., Smith, K.M., Lebrilla, C.B., Shelnut, J.A.: Application of matrix-assisted laser desorption/ionization Fourier transform mass spectrometry to the analysis of planar porphyrins and highly substituted nonplanar porphyrins. *Eur. Mass Spectrom.* **3**(6), 439–451 (1997)
42. Baykut, G., Jertz, R., Witt, M.: Matrix-assisted laser desorption/ionization Fourier transform ion cyclotron resonance mass spectrometry with pulsed in-source collision gas and in-source ion accumulation. *Rapid Commun. Mass Spectrom.* **14**(14), 1238–1247 (2000)
43. O'Connor, P.B., Costello, C.E.: A high pressure matrix-assisted laser desorption/ionization Fourier transform mass spectrometry ion source for thermal stabilization of labile biomolecules. *Rapid Commun. Mass Spectrom.* **15**(19), 1862–1868 (2001)
44. Baykut, G., Fuchser, J., Witt, M., Weiss, G., Gosteli, C.: A combined ion source for fast switching between electrospray and matrix-assisted laser desorption ionization in Fourier transform ion cyclotron resonance mass spectrometry. *Rapid Commun. Mass Spectrom.* **16**(17), 1631–1641 (2002)
45. O'Connor, P.B., Budnik, B.A., Ivleva, V.B., Kaur, P., Moyer, S.C., Pittman, J.L., Costello, C.E.: A high pressure matrix-assisted laser desorption ion source for Fourier transform mass spectrometry designed to accommodate large targets with diverse surfaces. *J. Am. Soc. Mass Spectrom.* **15**(1), 128–132 (2004)
46. Kutz, K.K., Schmidt, J.J., Li, L.J.: *In situ* tissue analysis of neuropeptides by MALDI FTMS in-cell accumulation. *Anal. Chem.* **76**(19), 5630–5640 (2004)
47. Stemmler, E.A., Bruns, E.A., Gardner, N.P., Dickinson, P.S., Christie, A.E.: Mass spectrometric identification of pEGFYSQRamide: a crustacean peptide hormone possessing a vertebrate neuropeptide Y (NPY)-like carboxy-terminus. *Gen. Comp. Endocrinol.* **152**(1), 1–7 (2007)
48. Stemmler, E.A., Cashman, C.R., Messinger, D.I., Gardner, N.P., Dickinson, P.S., Christie, A.E.: High-mass-resolution direct-tissue MALDI-FTMS reveals broad conservation of three neuropeptides (APSGFLGMRamide, GYRKPPFNGSIFamide and pQLLDHVFLRFamide) across members of seven decapod crustacean infraorders. *Peptides* **28**(11), 2104–2115 (2007)
49. Dickinson, P.S., Wiwatpanit, T., Gabranski, E.R., Ackerman, R.J., Stevens, J.S., Cashman, C.R., Stemmler, E.A., Christie, A.E.: Identification of SYWKQCAFNAVSCFamide: a broadly conserved crustacean C-type allatostatin-like peptide with both neuromodulatory and cardioactive properties. *J. Exp. Biol.* **212**(8), 1140–1152 (2009)
50. Verhaert, P.D.E.M., Pinkse, M., Prieto-Conaway, M.C.: Tissue imaging of neuropeptides by MALDI Orbitrap MS. In 57th American Society for Mass Spectrometry Conference on Mass Spectrometry and Allied Topics. Philadelphia, PA (2009)
51. Mize, T.H., Taban, I., Duursma, M., Seynen, M., Konijnenburg, M., Vijftigschild, A., Doornik, C.V., Rooij, G.V., Heeren, R.M.A.: A modular data and control system to improve sensitivity, selectivity, speed of analysis, ease of use, and transient duration in an external source FTICR-MS. *Int. J. Mass Spectrom.* **235**(3), 243–253 (2004)
52. Taban, L.M., van der Burgt, Y.E.M., Duursma, M., Takats, Z., Seynen, M., Konijnenburg, M., Vijftigschild, A., Attema, I., Heeren, R.M.A.: A novel workflow control system for Fourier transform ion cyclotron resonance mass spectrometry allows for unique on-the-fly data-dependent decisions. *Rapid Commun. Mass Spectrom.* **22**(8), 1245–1256 (2008)
53. Guo, X.H., Duursma, M., Al-Khalili, A., McDonnell, L.A., Heeren, R.M.A.: Design and performance of a new FT-ICR cell operating at a temperature range of 77–438 K. *Int. J. Mass Spectrom.* **231**(1), 37–45 (2004)
54. Mihalca, R., van der Burgt, Y.E.M., McDonnell, L.A., Duursma, M., Cerjak, I., Heck, A.J.R., Heeren, R.M.A.: Combined infrared multi-

- photon dissociation and electron-capture dissociation using co-linear and overlapping beams in Fourier transform ion cyclotron resonance mass spectrometry. *Rapid Commun. Mass Spectrom.* **20**(12), 1838–1844 (2006)
55. Rompp, A., Taban, I.M., Mihalca, R., Duursma, M.C., Mize, T.H., McDonnell, L.A., Heeren, R.M.A.: Examples of Fourier transform ion cyclotron resonance mass spectrometry developments: from ion physics to remote access biochemical mass spectrometry. *Eur. J. Mass Spectrom.* **11**(5), 443–456 (2005)
56. Aizikov, K., Smith, D.F., Chargin, D.A., Ivanov, S., Lin, T., Heeren, R.M.A., O'Connor, P.B.: Vacuum compatible sample positioning device for MALDI Fourier transform ion cyclotron resonance mass spectrometry imaging. In preparation. (2010)
57. Shaffer, S.A., Tang, K.Q., Anderson, G.A., Prior, D.C., Udseth, H.R., Smith, R.D.: A novel ion funnel for focusing ions at elevated pressure using electrospray ionization mass spectrometry. *Rapid Commun. Mass Spectrom.* **11**(16), 1813–1817 (1997)
58. Shaffer, S.A., Tolmachev, A., Prior, D.C., Anderson, G.A., Udseth, H.R., Smith, R.D.: Characterization of an improved electrodynamic ion funnel interface for electrospray ionization mass spectrometry. *Anal. Chem.* **71**(15), 2957–2964 (1999)
59. Ibrahim, Y., Tang, K.Q., Tolmachev, A.V., Shvartsburg, A.A., Smith, R.D.: Improving mass spectrometer sensitivity using a high-pressure electrodynamic ion funnel interface. *J. Am. Soc. Mass Spectrom.* **17**(9), 1299–1305 (2006)
60. Jiao, C.Q., Ranatunga, D.R.A., Vaughn, W.E., Freiser, B.S.: A pulsed-leak valve for use with ion trapping mass spectrometers. *J. Am. Soc. Mass Spectrom.* **7**(1), 118–122 (1996)
61. Mize, T.H., Amster, I.J.: Broad-band ion accumulation with an internal source MALDI-FTICR-MS. *Anal. Chem.* **72**(24), 5886–5891 (2000)
62. O'Connor, P.B., Costello, C.E.: Internal calibration on adjacent samples (INCAS) with Fourier transform mass spectrometry. *Anal. Chem.* **72**(24), 5881–5885 (2000)
63. Taban, I.M., McDonnell, L.A., Rompp, A., Cerjak, I., Heeren, R.M.A.: Simion analysis of a high performance linear accumulation octopole with enhanced ejection capabilities. *Int. J. Mass Spectrom.* **244**(2-3), 135–143 (2005)
64. Wilcox, B.E., Hendrickson, C.L., Marshall, A.G.: Improved ion extraction from a linear octopole ion trap: simion analysis and experimental demonstration. *J. Am. Soc. Mass Spectrom.* **13**(11), 1304–1312 (2002)
65. Caravatti, P., Allemann, M.: The infinity cell - a new trapped-ion cell with radiofrequency covered trapping electrodes for Fourier-transform ion-cyclotron resonance mass-spectrometry. *Org. Mass Spectrom.* **26**(5), 514–518 (1991)
66. Savard, G., Becker, S., Bollen, G., Kluge, H.J., Moore, R.B., Otto, T., Schweikhard, L., Stolzenberg, H., Wiess, U.: A new cooling technique for heavy-ions in a Penning trap. *Phys. Lett. A* **158**(5), 247–252 (1991)
67. Comisarow, M.B., Marshall, A.G.: Frequency-sweep Fourier transform ion cyclotron resonance spectroscopy. *Chem. Phys. Lett.* **26**(4), 489–490 (1974)
68. Jardin-Mathe, O., Bonnel, D., Franck, J., Wisztorski, M., Macagno, E., Fournier, I., Salzet, M.: MITICS (MALSI Imaging Team Imaging Computing System): a new open source mass spectrometry imaging software. *J. Proteomics* **71**(3), 332–345 (2008)
69. Guan, S.H., Marshall, A.G.: Stored waveform inverse Fourier transform (SWIFT) ion excitation in trapped-ion mass spectrometry: theory and applications. *Int. J. Mass Spectrom.* **157**, 5–37 (1996)
70. Gauthier, J.W., Trautman, T.R., Jacobson, D.B.: Sustained off-resonance irradiation for collisionactivated dissociation involving Fourier-transform mass-spectrometry - collision-activated dissociation technique that emulates infrared multiphoton dissociation. *Anal. Chim. Acta* **246**(1), 211–225 (1991)
71. Heck, A.J.R., Dekoning, L.J., Pinkse, F.A., Nibbering, N.M.M.: Mass-specific selection of ions in Fourier-transform ion-cyclotron resonance mass-spectrometry - unintentional off-resonance cyclotron excitation of selected ions. *Rapid Commun. Mass Spectrom.* **5**(9), 406–414 (1991)
72. Jeffries, J.B., Barlow, S.E., Dunn, G.H.: Theory of space-charge shift of ion cyclotron resonance frequencies. *Int. J. Mass Spectrom. Ion Process.* **54**, 169–187 (1983)
73. Francl, T.J., Sherman, M.G., Hunter, R.L., Locke, M.J., Bowers, W.D., McIver, R.T.: Experimental-determination of the effects of space-charge on ion-cyclotron resonance frequencies. *Int. J. Mass Spectrom. Ion Process.* **54**, 189–199 (1983)
74. Ledford Jr., E.B., Rempel, D.L., Gross, M.L.: Space charge effects in Fourier transform mass spectrometry mass calibration. *Anal. Chem.* **56**, 2744–2748 (1984)
75. Easterling, M.L., Mize, T.H., Amster, I.J.: Routine part-per-million mass accuracy for high- mass ions: space-charge effects in MALDI FT-ICR. *Anal. Chem.* **71**(3), 624–632 (1998)
76. Burton, R.D., Matuszak, K.P., Watson, C.H., Eyster, J.R.: Exact mass measurements using a 7 Tesla Fourier transform ion cyclotron resonance mass spectrometer in a good laboratory practices-regulated environment. *J. Am. Soc. Mass Spectrom.* **10**(12), 1291–1297 (1999)
77. Stafford, G.C., Taylor, D.M., Bradshaw, S.C., Syka, J.E.P. Enhanced sensitivity and dynamic range on an ion trap mass spectrometer with automatic gain control. In 35th ASMS Conference on Mass Spectrometry and Allied Topics. Denver, Co. (1987)
78. Belov, M.E., Zhang, R., Strittmatter, E.F., Prior, D.C., Tang, K., Smith, R.D.: Automated gain control and internal calibration with external ion accumulation capillary liquid chromatography-electrospray ionization-Fourier transform ion cyclotron resonance. *Anal. Chem.* **75**(16), 4195–4205 (2003)
79. Belov, M.E., Rakov, V.S., Nikolaev, E.N., Goshe, M.B., Anderson, G.A., Smith, R.D.: Initial implementation, of external accumulation liquid chromatography/electrospray ionization Fourier transform ion cyclotron resonance with automated gain control. *Rapid Commun. Mass Spectrom.* **17**(7), 627–636 (2003)
80. Senko, M., Zabrouskov, V., Lange, O., Wiegand, A., Horning, S.: LC/MS with external calibration mass accuracies approaching 100 ppb. In 52nd ASMS Conference on Mass Spectrometry and Allied Topics. Nashville, TN (2004)
81. Page, J.S., Bogdanov, B., Vilkov, A.N., Prior, D.C., Buschbach, M.A., Tang, K., Smith, R.D.: Automatic gain control in mass spectrometry using a jet disrupter electrode in an electrodynamic ion funnel. *J. Am. Soc. Mass Spectrom.* **16**(2), 244–253 (2005)
82. Jackson, S.N., Wang, H.Y.J., Woods, A.S.: Direct profiling of lipid distribution in brain tissue using MALDI-TOFMS. *Anal. Chem.* **77**(14), 4523–4527 (2005)
83. Jackson, S.N., Wang, H.-Y.J., Woods, A.S., Ugarov, M., Egan, T., Schultz, J.A.: Direct tissue analysis of phospholipids in rat brain using MALDI-TOFMS and MALDI-ion mobility-TOFMS. *J. Am. Soc. Mass Spectrom.* **16**(2), 133–138 (2005)
84. Jackson, S.N., Wang, H.-Y.J., Woods, A.S.: *In situ* structural characterization of phosphatidylcholines in brain tissue using MALDI-MS/MS. *J. Am. Soc. Mass Spectrom.* **16**(12), 2052–2056 (2005)
85. Ma, X., Liu, G., Wang, S., Chen, Z., Lai, M., Liu, Z., Yang, J.: Evaluation of sphingolipids changes in brain tissues of rats with pentylentetrazol-induced kindled seizures using MALDI-TOF-MS. *J. Chromatogr. B* **859**(2), 170–177 (2007)
86. Astigarraga, E., Barreda-Gomez, G., Lombardero, L., Fresnedo, O., Castano, F., Giralt, M.T., Ochoa, B., Rodriguez-Puertas, R., Fernandez, J.A.: Profiling and imaging of lipids on brain and liver tissue by matrix-assisted laser desorption/ionization mass spectrometry using 2-mercaptobenzothiazole as a matrix. *Anal. Chem.* **80**(23), 9105–9114 (2008)
87. Klinkert, I., McDonnell, L.A., Luxembourg, S.L., Altelaar, A.F.M., Amstalden, E.R., Piersma, S.R., Heeren, R.M.A.: Tools and strategies for visualization of large image data sets in high-resolution imaging mass spectrometry. *Rev. Sci. Instrum.* **78**(5), 1–10 (2007)
88. Marshall, A.G., Guan, S.H.: Advantages of high magnetic field for Fourier transform ion cyclotron resonance mass spectrometry. *Rapid Commun. Mass Spectrom.* **10**(14), 1819–1823 (1996)
89. Makarov, A., Denisov, E., Lange, O.: Performance evaluation of a high-field orbitrap mass analyzer. *J. Am. Soc. Mass Spectrom.* **20**(8), 1391–1396 (2009)